

Supporting Information  
**Imaging mechanical vibrations in suspended graphene sheets**

D. Garcia-Sanchez, A. M. van der Zande, A. San Paulo, B. Lassagne, P. L. McEuen and A. Bachtold

**A - Sample fabrication**

Suspended graphene sheets are fabricated by mechanical exfoliation. A freshly cleaved piece of Kish graphite (Toshiba Ceramics) is rubbed onto a degenerately doped silicon wafer with 290 nm SiO<sub>2</sub> grown by plasma enhanced chemical vapor deposition. Before depositing the graphene, the wafer is patterned with trenches using photolithography and plasma etching. The trenches are millimeter long, 0.5 – 10 μm wide, and 250 nm deep. Electrodes defined by photolithography between the trenches are deposited using electron-beam evaporation and consist of 5 nm Cr and 35 nm Au.

**B- Description of the FEM model**

To model the shape of the eigenmodes, we have developed a simulation based on finite element methods (FEM) using ANSYS. The first step of the simulation is to account for the buckling of the suspended sheet by finding the adequate boundary conditions at the clamping edges. To do this, we hold one clamping edge of the suspended region fixed, and impose an in plane displacement to the other clamping edge. Specifically, the displacement of this edge consists of a translation and a rotation within the undeformed resonator surface. Since the resulting out of plane displacement can be large, calculations are carried out taking into account geometric non-linear deformations<sup>1</sup>. To ensure that the buckling goes in the desired direction, we apply an out of plane perturbative force, which is then cleared at the end of the calculations. We make the assumption that the mechanical properties of the resonator are isotropic with 1TPa for the Young's modulus and 0.17 for the Poisson ratio<sup>2</sup>. The exact value of the Poisson ratio has little effect on the output of the calculations. In the second step of the simulation, a modal analysis is performed to determine the resonance frequency and the eigenmode shape of the deformed resonator. Here, the modal analysis is carried out in the linear regime because the amplitude of the vibration is small. To check that this simulation is free of errors, it has been successfully compared to analytical predictions for a beam under tension<sup>3</sup>. The simulation also reproduces recent calculations on nanotubes with slack<sup>4</sup>. See sections C and D.

### C- Comparison between the FEM model and analytical expressions for resonators under tension.

The resonance frequency for a beam under weak uniform tension ( $T \ll EI/l^2$ ) is<sup>5</sup>

$$f_1 = \frac{22.4}{2\pi l^2} \sqrt{\frac{EI}{\rho w t}} + \frac{0.28}{2\pi} T \sqrt{\frac{1}{\rho w t EI}} \quad (1)$$

We take the length  $l = 500$  nm, the width  $w = 20$  nm, the thickness  $t = 3.5$  Å, the density  $\rho = 2200$  kg/m<sup>3</sup>, and the Young's Modulus  $E = 1$  TPa. The bending moment of a rigid beam is  $I = wt^3/12$ .

For high tension ( $T \gg EI/l^2$ ) the frequency can be expressed as<sup>3</sup>

$$f_1 = \frac{1}{2l} \sqrt{\frac{T}{\rho w t}} \left[ 1 + 2\xi + (4 + \pi^2 / 2)\xi^2 \right] \quad (2)$$

with  $\xi^2 = Etw^3 / 12Tl^2$ .

Figure S1 shows the resonance frequency as a function of tension using the FEM model and the above expressions. There is a good agreement between the theory and the FEM model.

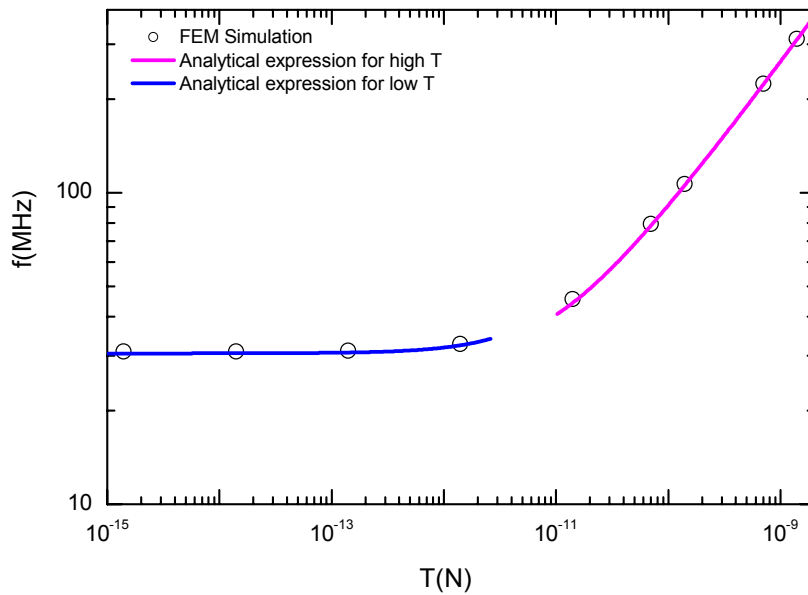


**Figure S1** Resonance frequency as a function of tension for the first eigenmode of a graphene resonator under tension.

### D- Comparison between the FEM model and previous simulations on buckled SWNTs.

Previous work<sup>4</sup> has reported numerical studies on SWNT resonators that are buckled (slack). We compare this work to the FEM model that we have developed. For this, we use the same geometry and the same physical

characteristics as in reference 4. The resonator is a doubly clamped rod with  $l=1.75\mu\text{m}$ ,  $d=2\text{nm}$ ,  $E=2.18\text{TPa}$ ,  $\rho=2992\text{kg/m}^3$  and a slack of 0,3%. The slack is defined as the ratio of the excess length of the tube to the distance between the clamping points. Figure S2 shows the resonance frequency for different eigenmodes obtained with the two simulation techniques. A good agreement is obtained.

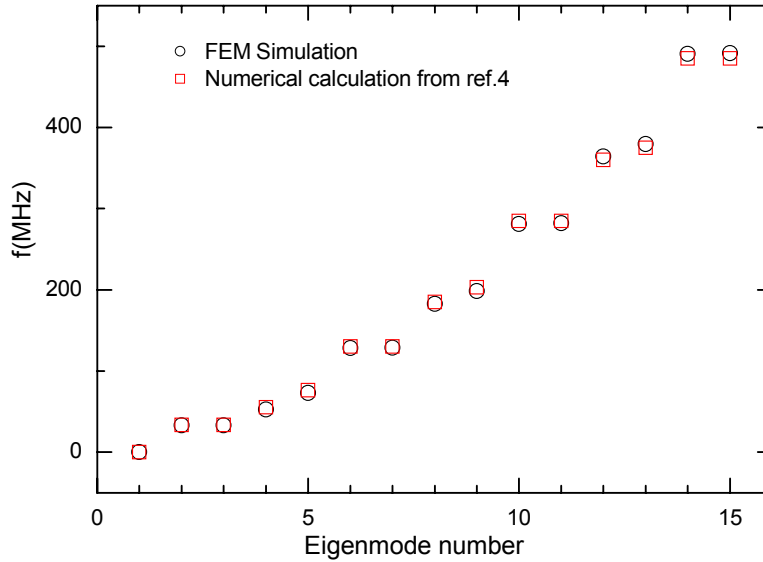


**Figure S2** Resonance frequency for different eigenmodes of a SWNT resonator with 0.3% of slack.

**Conclusions of sections C and D.** The FEM model shows a good agreement with established analytical expressions for beam resonators under tension and previous numerical calculations on buckled SWNTs. Note that the FEM model that we have developed can go beyond these cases. The model can be applied to resonators with any arbitrary geometry and any arbitrary stressed state.

**E- SFM detection of mechanical vibrations.**

We have developed a technique based on scanning force microscopy (SFM) to detect the mechanical vibrations of nanotube and graphene resonators<sup>6</sup>. The resonator motion is electrostatically actuated with an oscillating voltage applied on a gate electrode. The frequency  $f_{RF}$  of the driving voltage  $V_{RF}$  is set at (or close to) the resonance frequency of the resonator. In addition,  $V_{RF}$  is modulated at  $f_{mod}$ ,  $(1 - \cos(2\pi f_{mod}t)) \cos(2\pi f_{RF}t)$ . While the SFM cantilever cannot follow the rapid oscillations at  $f_{RF}$ , it can detect the modulation envelope.

The topography imaging is obtained in tapping mode using the second eigenmode of the SFM cantilever. The vibrations are detected with the first eigenmode of the SFM cantilever. Figure S3 shows that the signal of the vibrations is significantly enhanced when  $f_{mod}$  is matching the resonance frequency  $f_{ip}$  of the first eigenmode of the SFM cantilever. As a result, measurements are carried out with  $f_{mod} = f_{ip}$ .

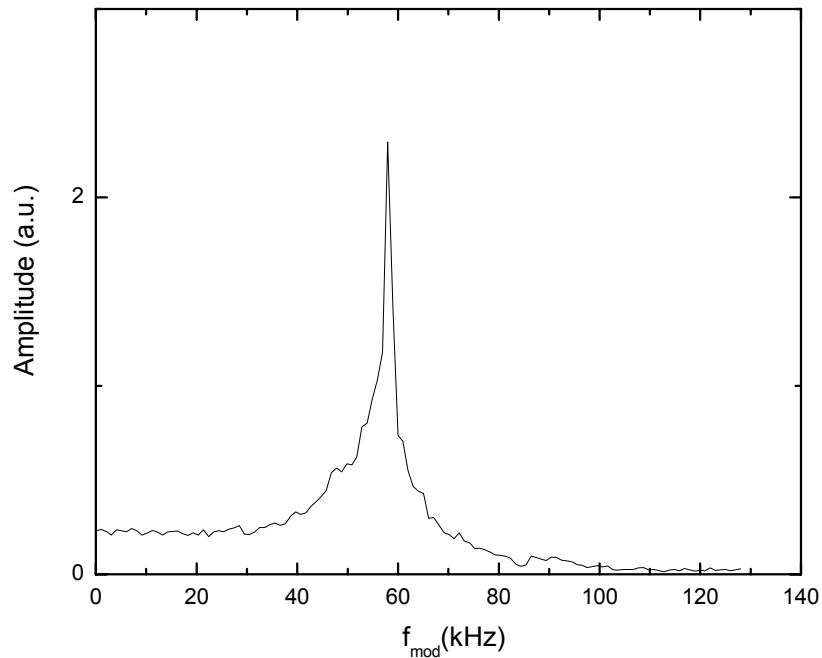


**Figure S3** Detected response of the vibration of a nanotube driven at resonance as a function of  $f_{mod}$ . The frequency of the first eigenmode of the SFM cantilever is 58 kHz. Nanotube resonance frequency  $f_{RF}$  is 153 MHz. Measurements are taken at the nanotube position where the vibration amplitude is maximum.

Graphene resonators show a lorentzian response to the rf drive frequency. Figure S4 a shows the frequency response of a graphene resonator measured with the SFM technique. For comparison, Fig. S4 b shows the frequency response of the same resonator measured using optical interferometry<sup>7</sup>. The resonance frequencies are very similar for both techniques. However, the quality factor measured with the SFM technique is much lower due to energy dissipation to air, as the SFM technique is operated at atmospheric conditions, while the optical interferometry is performed in vacuum. Note that the low Q is not attributed to the disturbance of the SFM tip<sup>6</sup>. Indeed, we have noticed no change in the quality factor as the amplitude set point of the SFM cantilever is reduced by 3%–5% from the limit of cantilever retraction, which corresponds to the enhancement of the resonator-tip interaction.

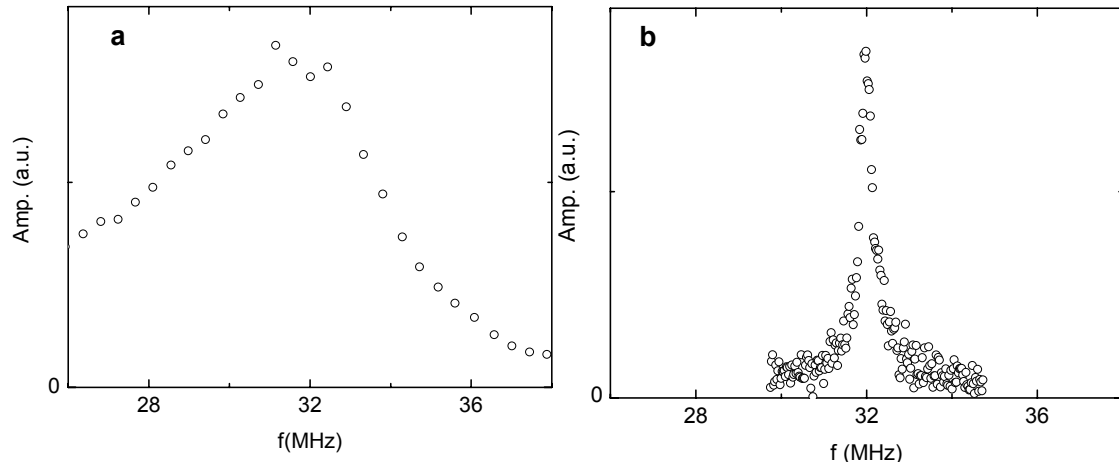


**Figure S4** **a** Resonance peak of the fundamental mode of the graphene resonator shown in Figure 2 of the paper. The measurement is carried out using the SFM technique in air. The resonance is found at  $\sim 31$  MHz with the quality factor  $Q = 5$ . Measurements are taken at the position where the vibration amplitude is maximum. **b** Resonance peak measured optically with a pressure of  $< 10^{-6}$  torr. The resonance is found at 32 MHz with  $Q = 64$ .

As shown in Eq. 1 of the paper, the radio frequency force  $F_{RF}$  on the suspended sheet is a linear function of the offset voltage  $V_{DC}$  and the radio frequency voltage  $V_{RF}$ . Figure S5 shows vibration amplitude as a function of  $V_{DC}$  for an edge eigenmode of a graphene resonator. We find that the vibration amplitude is a linear function of the DC voltage and thus of the force. By operating in this regime, we ensure that the resonators are operating in the linear response regime, and the exotic edge eigenmodes are not a result of non-linear effects.

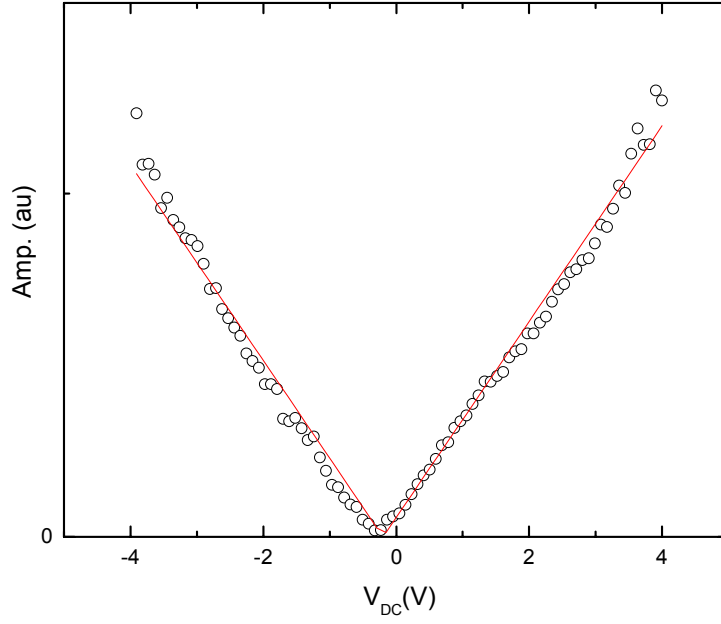


**Figure S5** Vibration amplitude as a function of  $V_{DC}$  at  $f_l = 33$  MHz and  $V_{RF} = 100$  mV for an edge eigenmode of a graphene resonator. The dimensions of the suspended sheet are  $t = 6$  nm and  $l = 3.5$   $\mu$ m. The measurements are obtained at the position of the graphene sheet where the amplitude is maximum

#### F- Estimation of the vibration amplitude of graphene resonators.

The amplitude of the vibration can be estimated when considering beams that neither have slack nor tension.

The eigenfunctions  $U_n(x)$  are obtained from<sup>6,8</sup>:

$$\rho A \frac{\partial^2 U_{beam}}{\partial t^2} + EI \frac{\partial^4 U_{beam}}{\partial x^4} = 0 \quad (4)$$

The displacement of the resonator can be expanded in terms of  $U_n(x)$ ,

$$z_{beam} = \left| \sum \alpha_n U_n \exp(-i2\pi f_{RF} t) \right| \quad (5)$$

where

$$\alpha_n = \frac{1}{4\pi^2 A \rho L^3} \frac{1}{f_n^2 - f_{RF}^2 - i f_n^2 / Q_n} \int_0^l U_n(x) F_{RF}(x) dx \quad (6)$$

with  $f_n$  the eigenfrequencies,  $Q_n$  the quality factor for each eigenmode and

$F_{RF} = \partial C(x) / \partial(z)(V_{DC} - \phi)V_{RF}$ .  $C(x)$  is the capacitance per unit of length and is given by  $C(x) = \epsilon_0 w / z$

with  $w$  the width of the resonator and  $z$  the separation between the resonator and the gate. We have estimated

that the maximum amplitude of the graphene resonator in Figure 2 of the paper is 0.1 nm. For this, we have used  $Q = 5$ ,  $V_{DC} - \phi = 3V$ , and  $V_{RF} = 60$  mV.

1 Zienkiewicz, O.C.; Taylor, R.L. *The Finite Element Method 5th edition*. Butterworth-Heinemann; Oxford, 2000.

2 Popov, V.N.; Van Doren, V.E.; Balkanski M. Elastic properties of single-walled carbon nanotubes. *Phys. Rev. B* **2000**, *61*, 3078.

3 E. Buks, M.L. Roukes, *Phys. Rev. B* **2001**, *63*, 033402.

4 Üstünel, H., Roundy, D.; Arias. T.A. *Nano Lett.* **2005**, *5*, 523.

5 S. Sapmaz, *et al.*, *Phys. Rev. B* **2003**, *67*, 235414.

6 Garcia-Sanchez, D.; *et al.* *Phys. Rev. Lett.* **2007**, *99*, 085501.

7 Bunch, J.S.; *et al.* *Science* **2007**, *315*, 490.

8 A. N. Cleland., *Foundations of Nanomechanics* (Springer, Berlin, 2003).